May 2000 • NREL/SR-520-28375

Subcontractor Report

Atmospheric Pressure Chemical Vapor Deposition of CdTe for High Efficiency Thin Film PV Devices

Annual Subcontract Report
26 January 1999 — 25 January 2000

P.V. Meyers
ITN Energy Systems, Wheat Ridge, Colorado

R. Kee, C. Wolden, J. Kestner, L. Raja,
V. Kaydanov, T. Ohno, and R. Collins
Colorado School of Mines, Golden, Colorado

A. Fahrenbruch
ALF, Inc., Stanford, California

National Renewable Energy Laboratory

1617 Cole Boulevard
Golden, Colorado 80401-3393

NREL is a U.S. Department of Energy Laboratory
Operated by Midwest Research Institute • Battelle • Bechtel

Contract No. DE-AC36-99-GO10337

May 2000 • NREL/SR-520-28375

Atmospheric Pressure Chemical Vapor Deposition of CdTe for High Efficiency Thin Film PV Devices

Annual Subcontract Report
26 January 1999 — 25 January 2000

P.V. Meyers
ITN Energy Systems, Wheat Ridge, Colorado

R. Kee, C. Wolden, J. Kestner, L. Raja,
V. Kaydanov, T. Ohno, and R. Collins
Colorado School of Mines, Golden, Colorado

A. Fahrenbruch
ALF, Inc., Stanford, California

NREL Technical Monitor: H.S. Ullal

Prepared under Subcontract No. ZAK-8-17619-03

National Renewable Energy Laboratory

1617 Cole Boulevard
Golden, Colorado 80401-3393

NREL is a U.S. Department of Energy Laboratory
Operated by Midwest Research Institute • Battelle • Bechtel

Contract No. DE-AC36-99-GO10337

NOTICE

Available electronically at http://www.doe.gov/bridge

Available for a processing fee to U.S. Department of Energy
and its contractors, in paper, from:

U.S. Department of Energy
Office of Scientific and Technical Information
P.O. Box 62
Oak Ridge, TN 37831-0062
phone: 865.576.8401
fax: 865.576.5728
email: reports@adonis.osti.gov

Available for sale to the public, in paper, from:

U.S. Department of Commerce
National Technical Information Service
5285 Port Royal Road
Springfield, VA 22161
phone: 800.553.6847
fax: 703.605.6900
email: orders@ntis.fedworld.gov
online ordering: http://www.ntis.gov/ordering.htm

Printed on paper containing at least 50% wastepaper, including 20% postconsumer waste

Title: **Atmospheric Pressure Chemical Vapor Deposition of CdTe for High Efficiency Thin Film PV Devices**

Organization: ITN Energy Systems, 12401 West 49th Ave., Wheat Ridge, CO 80033

Principal Investigator: Peter V. Meyers (303-285-5135)

Key Personnel: R. Kee†, C. Wolden†, J. Kestner†, L. Raja†, V. Kaydanov†, T. Ohno†, R. Collins†, A. Fahrenbruch‡

† Colorado School of Mines, Golden, CO

‡ALF, Inc., Stanford, CA

Abstract: ITN's three year project Atmospheric Pressure Chemical Vapor Deposition (APCVD) of CdTe for High Efficiency Thin Film PV Devices has the overall objectives of improving thin film CdTe PV manufacturing technology and increasing CdTe PV device power conversion efficiency. CdTe deposition by APCVD employs the same reaction chemistry as has been used to deposit 16% efficient CdTe PV films, i.e., close spaced sublimation, but employs forced convection rather than diffusion as a mechanism of mass transport. Tasks of the APCVD program center on demonstration of APCVD of CdTe films, discovery of fundamental mass transport parameters, application of established engineering principles to the deposition of CdTe films, and verification of reactor design principles which could be used to design high throughput, high yield manufacturing equipment. Additional tasks relate to improved device measurement and characterization procedures that can lead to a more fundamental understanding of CdTe PV device operation and ultimately to higher device conversion efficiency and greater stability. Under the APCVD program, device analysis goes beyond conventional one-dimensional device characterization and analysis toward two dimension measurements and modeling. Accomplishments of the second year of the APCVD subcontract include: deposition of the first APCVD CdTe; identification of deficiencies in the first generation APCVD reactor; design, fabrication and testing of a "simplified" APCVD reactor; deposition of the first dense, adherent APCVD CdTe films; fabrication of the first APCVD CdTe PV device; modeling effects of CdSTe and SnO_x layers; and electrical modeling of grain boundaries.

Table of Contents

1 Project objective 3

2 Approach 3

2.1 Deposition technology 3

2.2 Device analysis 4

3 APCVD of CdTe 4

3.1 Reactor design and testing – first year accomplishments 4

3.2 Pre-deposition reactor modifications 4

3.3 First CdTe deposition 5

3.3.1 Description of Deposition Run 5

3.3.2 First CdTe film 5

3.4 Post-deposition reactor modifications – simplified reactor 6

3.4.1 Leaks 7

Non-uniform gas flow 7

3.4.3 Deposition of CdTe onto showerhead 8

3.4.4 Substrate temperature control 8

3.4.5 Dust formation 8

Dry Runs – simplified reactor 8

3.4.7 APCVD CdTe Films and Devices – simplified reactor 9

3.4.8 Next Steps - Simplified Reactor 10

4 Modeling of CdS/CdTe thin film solar cells 10

4.1 Device characterization and analysis 10

4.2 AMPS Modeling of CdTe/CdS thin film PV devices 11

4.2.1 Purposes of modeling 11

Addition of a CdS_XTe_{1-X} alloy layer 13

4.2.3 SnO_X Window layer 14

4.2.4 AMPS grain boundary simulation 16

4.2.5 AMPS modeling conclusions 17

5 Summary 17

5.1 Phase II Summary 17

5.2 Planned Phase III activities 18

5.3 Planned third year milestones 18

6 References 18

1 Project objective

ITN's three year project Atmospheric Pressure Chemical Vapor Deposition (APCVD) of CdTe for High Efficiency Thin Film PV Devices has the overall objectives of improving thin film CdTe photovoltaic (PV) manufacturing technology and increasing CdTe PV device power conversion efficiency. Tasks required to accomplish the overall goals are grouped into 1) development of APCVD apparatus and procedures which enable controlled deposition of device-quality film over large areas and 2) development of advanced measurement and analytical procedures which provide useful and effective device characterization.

2 Approach

CdTe deposition by APCVD employs the same reaction chemistry as has been used to deposit 16% efficient CdTe PV films[1,2], i.e., close spaced sublimation (CSS), but employs forced convection rather than diffusion as a mechanism of mass transport. Tasks of the APCVD program center on 1) demonstration of APCVD of CdTe films, 2) discovery of fundamental mass transport parameters, 3) application of established engineering principles to the deposition of CdTe films and, 4) verification of the reactor design principles which could be used to design high-throughput, high-yield manufacturing equipment. Additional tasks relate to improved device measurement and characterization procedures which can lead to a more fundamental understanding of CdTe PV device operation. Specifically, under the APCVD program, device analysis goes beyond conventional one-dimensional device characterization and analysis toward two-dimension measurements and modeling.

2.1 Deposition technology

Although there are many demonstrated methods for producing high-efficiency CdTe solar cells, large-scale commercial production of thin-film CdTe PV modules has not yet been realized.[3] An important contributor to the commercial production of thin-film CdTe will be development of advanced deposition reactors. APCVD represents a generation beyond CSS. APCVD combines proven CSS reaction chemistry with state-of-the-art engineering principles to enable design of thin film deposition reactors for the manufacturing environment. APCVD's anticipated advantages include:

- Low equipment cost compared to vacuum processing because equipment will need neither the structural strength nor the pumping systems of a vacuum chamber.
- Large area uniformity achieved through control of temperature and gas flow - both of which are subject to rigorous engineering design.
- Simplified process control and source replenishment because the source gas generation is physically separated from the deposition chamber.
- CdTe PV device fabrication process compatibility in that APCVD is presently used commercially to deposit transparent conducting oxide (TCO) films commonly used in CdTe solar cells. In fact, the processing sequence: deposit TCO, deposit CdS, deposit CdTe, dry $CdCl_2$ heat treatment and metalorganic CVD of electrodes could be performed in a single continuous process.
- Low raw material costs as CdTe is used in its least expensive form - chunks.
- Simplified continuous processing because gas curtains replace load locks.

2.2 Device analysis

Operation of thin film PV devices is normally analyzed in one dimension – distance perpendicular to the device surface. One dimensional (1D) modeling is justified in that thin film PV devices are basically comprised of a stack of thin films of various compositions and properties and through which light and electricity flow in a direction essentially perpendicular to the plane of the films. There is no question that 1D modeling successfully describes the fundamentals of thin film PV device operation. Nonetheless, quantitative analyses of PV device operation, its dependence on device fabrication procedures, and factors affecting stability in the field have not been achieved. Furthermore, we know that individual films are not homogeneous, but rather are comprised of grains. Each grain is surrounded by grain boundaries that are oriented in all directions and which have different physical, electrical and optical properties than the interior of the grain. Tasks of this program are directed toward techniques that quantify the properties of grain boundaries and the effects grain boundaries have on thin film PV device operation.

An important distinction between the commonly used one dimensional (1D) models and a two dimensional (2D) model is that the 2D model allows for electric fields and carrier transport both parallel and perpendicular to the direction from which light is incident. These perpendicular components are brought about by differences in carrier type, carrier concentration, and carrier lifetime associated with grain boundaries. In this project efforts are being directed toward identification and application of experimental techniques for characterization of grain boundaries and the investigation of the relationships between grain boundary characteristics and operating properties of working devices. An important aspect of this approach is maintenance of a close connection between measurement, modeling and analysis.

3 APCVD of CdTe

3.1 Reactor design and testing – first year accomplishments

During the first year of the program the concept of APCVD of CdTe underwent rigorous evaluation by the combined ITN/CSM scientific and engineering team and the apparent practical advantages of APCVD over state-of-the-art manufacturing techniques withstood this scrutiny. Furthermore, a first generation APCVD reactor was designed, built and evaluated through performance of "dry runs", i.e., operating without CdTe. Specific first year accomplishments included:

- Selection of the Stagnant Flow Reactor design concept
- Development of a detailed reactor design
- Performance of detailed numerical calculations simulating reactor performance
- Fabrication and installation of an APCVD reactor
- Performance of dry runs to verify reactor performance

Nonetheless, at the end of year one of the program APCVD's apparent advantages had not been demonstrated.

3.2 Pre-deposition reactor modifications

Dry runs performed during the first year of the program identified deficiencies in reactor design that indicated certain design modifications. Modifications made at the beginning of the second year of the program included: 1) installation of a custom nozzle heater, 2) installation of alumina disperser plates designed to produce more uniform source gas flow from the nozzle, 3) installation a Lexan enclosure around the APCVD reactor, 4) replacement of appropriate pressure sensors, and 5) installation of a pressure sensor activated solenoid valve which cuts off gas flow to the reactor if internal reactor pressure exceeds ambient pressure.

During the course of various system testing procedures problems were encountered with leaks in the system, broken glassware, blown fuses and a burned out gas preheater. In each case where problems were encountered, the condition was corrected not by a simple repair but rather by design and installation of improved, more robust system hardware. Thus, at the end of the sixth quarter the APCVD reactor system had been rebuilt and reassembled, APCVD operating procedures had been written, and the system had passed a health, safety and environmental inspection by the Environmental Health Manager at CSM. Figure 1 is a schematic drawing of the APCVD reactor at the middle of Phase II.

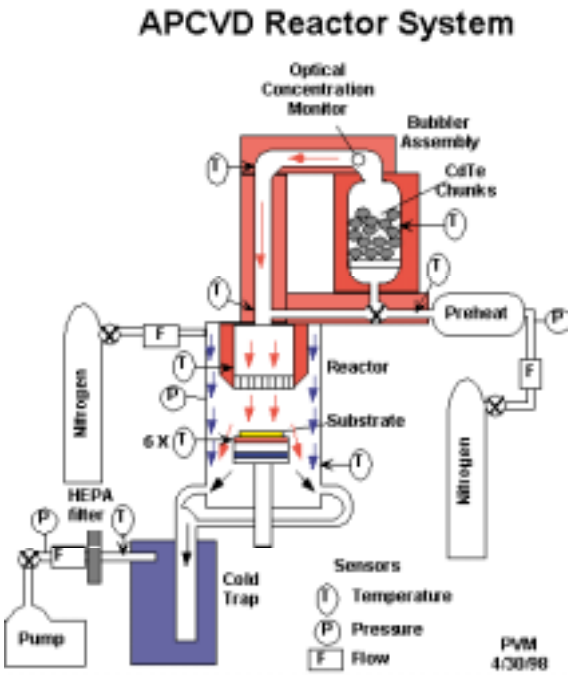

Figure 1. Schematic of original APCVD reactor.

3.3 First CdTe deposition

On August 26th we performed the first CdTe deposition in the APCVD reactor. All equipment – temperature controllers, power controllers, temperature and flow sensors, data acquisition unit, exhaust blowers, etc. - operated as designed. In addition to recording temperature and flow data using a data acquisition unit, the entire deposition was recorded on videotape.

3.3.1 Description of Deposition Run

All zones – bubbler, nozzle, hot piping, and substrate – were heated to operating temperature. CdTe source temperature was set to 725°C – corresponding to a source vapor pressure, i.e., combined partial pressures of Cd(g) + Te_2(g), of ~0.5 torr. Due to concerns over chemical reaction between thermocouple wires and the hot Te_2(g), substrate temperature was not measured directly but was estimated based on data obtained during dry runs. Estimated temperature of the back surface of the substrate was 600°C. The top surface, i.e., the substrate surface upon which the film was deposited, may have been several tens of degrees hotter. The substrate was LOF 3mm Tec 8 glass (3 mm thick SnO_2:F-coated sodalime glass with electrical conductivity of ~8Ω/□) with no CdS.

Prior to directing the source carrier gas through the CdTe bubbler, i.e., while carrier gas flow was still directed through bypass tubing (see Figure 1) and therefore before CdTe deposition was expected to begin, a white deposit began to form on the substrate. Later analysis, described below, indicated that the white deposit was TeO_2. In spite of the presence of the white deposit, the run proceeded as planned. CdTe source gas was turned on (i.e., preheated nitrogen gas was directed through the CdTe bubbler) for about 10 minutes during which time a black deposit of CdTe formed on the substrate. Also noted during the run was formation of fine, black powder – presumably created by homogeneous nucleation of CdTe in the gas phase.

3.3.2 First CdTe film

SEM and Auger analysis were used to characterize the CdTe deposition. A key issue was to determine whether the ambient pressure and method of mass transport affect the nature of the deposited films. Recall that APCVD of CdTe is similar to CSS of CdTe in that both processes involve 1) sublimation of

Cd and Te_2 gasses from hot CdTe, 2) transport of the source gasses to a hot substrate, and 3) deposition of CdTe films. The main difference between the two processes is step #2 - that CSS takes place at low pressure (~40 torr) and that mass transport of the source gasses is by diffusion whereas APCVD occurs at atmospheric pressure and relies on forced convection to transport the source gasses. A fundamental premise of the APCVD program has been that APCVD films have the same reaction chemistry as do CSS films, i.e., that the films with the same physical and electrical properties can be grown by either technique. If APCVD can indeed produce the same quality films as CSS, then the engineering advantages of APCVD – i.e., low equipment cost, large area uniformity, etc. – can be used to make the same high efficiency devices obtained in laboratory scale CSS equipment but on a larger, industrial scale.

SEM photographs taken at NREL by Rick Matson and displayed in Figure 2 show that the first CdTe films grown by APCVD at ITN/CSM show similar structure – although on a larger scale – to films deposited at NREL by CSS on a 645°C substrate. As described above, substrate temperature during the first APCVD run was not known, but 645°C is within the range of reasonable estimates. The similarity in structure between the APCVD and CSS films strongly suggests that the reaction chemistry and growth of APCVD films is similar to that of CSS films

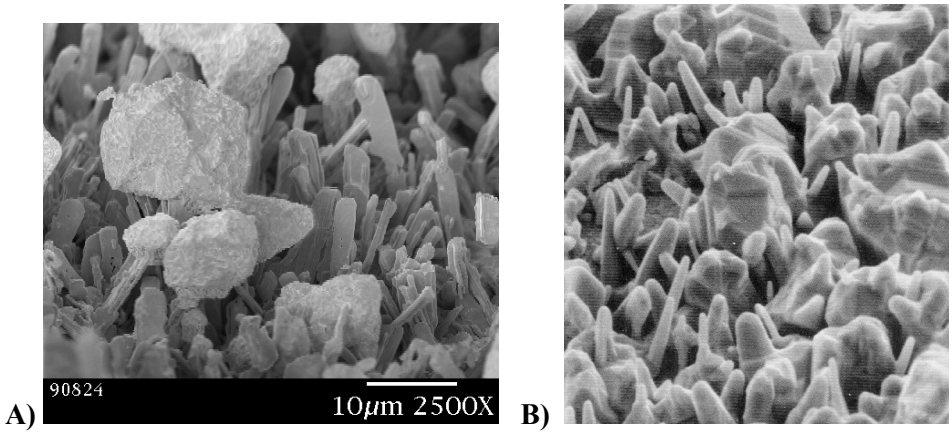

Figure 2. Comparison of microstructure of films grown A) by APCVD at ITN/CSM (Run #90826) and B) by CSS at NREL at 645°C (X. Li et al., Proc. 25th IEEE PVSC, pp 933-936). Magnification of the right-hand photo (CSS at NREL) is approximately six times that of the left-hand photo (APCVD at ITN).

Auger analysis performed by Amy Swartzlander, NREL, and XPS analysis by Tim Ohno identified the white deposits in these first APCVD CdTe films as TeO_2. As there was no intentional oxygen in the source or carrier gasses – which were both industrial grade nitrogen, TeO_2 in the films suggested to researchers that there were leaks in the reactor that allowed relatively humid room air to affect reactor performance and film growth. Thus, although the initial CdTe deposition supported the fundamental premise of the APCVD program, further experimentation would be required in order to develop operating procedures to deposit device quality films.

3.4 Post-deposition reactor modifications – simplified reactor

Several reactor design issues were raised by the first CdTe deposition run. White films and powder were observed even while the CdTe bubbler temperature was below that expected to form Cd and Te_2 vapors, deposition was non-uniform to the extent that some areas of the film were white while others were black, a black deposit – probably CdTe – formed on the showerhead, substrate temperature control was inadequate, dust particles formed in the reactor above the substrate, and films deposited on reactor windows.

3.4.1 Leaks

For reasons of safety and environmental control, the bubbler is operated at below ambient room pressure. Thus leaks in the reactor allow room air to mix with the source and curtain gasses and to affect source gas generation and film growth. It is believed that the presence of white TeO_2 powder prior to intentional film deposition was the result of leaks upstream of the bubbler that allowed room air to be drawn through the bubbler by the lower pressure downstream in the reaction chamber. Leaks in the reactor were addressed through design of a simplified bubbler and through improved high temperature stainless steel to quartz joints.

One concession made in order to reduce leaks in the new design is that the provision for source gas bypass of the bubbler has been eliminated. Provision for the source gas to bypass the bubbler had been included so that the substrate temperature and other reactor operating conditions could be established at steady state conditions prior to introducing the Cd and Te_2 source gasses. Unfortunately the bypass tubing included a two-position valve that had to operate at ~700°C and which is suspected to have been a major source of leaks. It is believed that operating procedures for the simplified bubbler can be developed which minimize effects of this design change and which will enable deposition of device quality films. Later generations of reactor design will be developed to produce steady state conditions within the APCVD reactor deposition zone.

3.4.2 Non-uniform gas flow

During the first "live" run deposition was highly non-uniform. Swirling dust was observed in the reaction zone and black deposits formed on the reactor windows – see Figure 3. Analysis of the deposition patterns suggested that neither the curtain gas flow nor the nozzle flow through the showerhead were uniform. Deposition of black films on the reactor windows was attributed to eddies in the curtain gas flow. In the modified design curtain gas flow is controlled through installation of baffles which restrict flow to defined channels rather than allowing gas to flow freely throughout all of the open space between the nozzle heater and reactor walls.

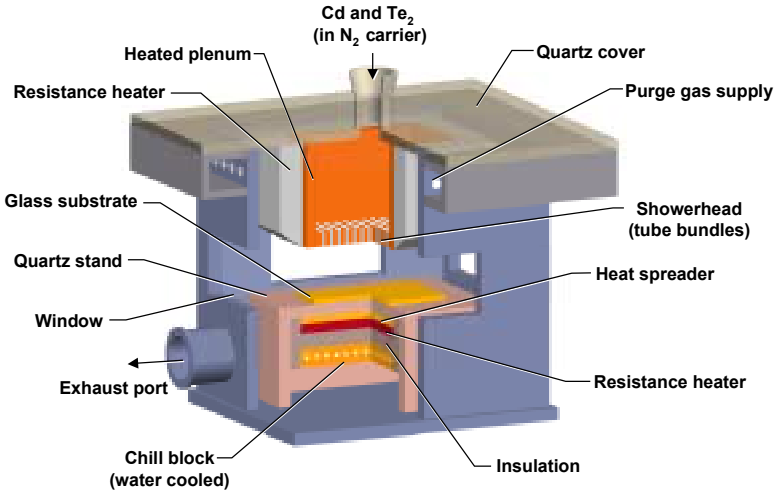

Figure 3. Sketch showing essential elements of APCVD reactor deposition chamber.

At least part of the non-uniformity of the source gas flow through the showerhead was attributed to breakage of one of the alumina disperser plates - discovered after the run had been completed. In the modified design showerhead flow will be made uniform by using a specially designed alumina sheet with multiple, sub-millimeter diameter holes. At typical source gas flow rates, pressure drop across the alumina plate is sufficient to produce uniform flow without the necessity of flow baffles inside the nozzle.

3.4.3 Deposition of CdTe onto showerhead

During CdTe deposition the showerhead at the bottom of the nozzle became coated with a black deposit - apparently CdTe. Deposition onto the showerhead had not been expected as data collected during dry runs indicated that showerhead temperature would be about 40°C above the expected source saturation temperature. Nonetheless, subsequent thermal analysis of the showerhead did predict large thermal gradients across the surface. Bob Kee developed a thermal model of a simplified showerhead – comprised of a single alumina plate as described above – which indicates that temperature would be fairly uniform across the entire showerhead surface. Elimination of the flow baffles from within the nozzles, as described above, is an important contributor to showerhead temperature uniformity.

3.4.4 Substrate temperature control

During previous runs the substrate heater did not achieve set point temperature although it was operated continuously at maximum power. Especially in view of the absence in the new design of the ability to preheat the substrate with bypassed source gas, provisions were made to increase power to the substrate heater by about 20%.

3.4.5 Dust formation

During CdTe deposition dust was generated within the deposition zone apparently due to mixing of the room temperature curtain gas with the ~750°C Cd and Te_2-laden source gas in eddies which swirled above the substrate. Eddies can be reduced or eliminated through design of streamline flow baffles that separate the cool curtain gas from the hot source gas until after the source gas has passed across the substrate. James Kestner has taken a one-week course taught by the software vendor in Huntsville, AL on application of CFD-ACE, a commercially available computer software program that solves the 3D Navier-Stokes equations governing fluid flow and associated physics. James, with guidance from his advisor Colin Wolden, will utilize this gas flow modeling capability to design flow baffles for the modified APCVD reactor. In the meantime, a heuristic baffle design was built and installed in the reaction chamber.

3.4.6 Dry Runs – simplified reactor

Upon completion of the reactor modifications described above, a set of dry runs was performed in order to evaluate and quantify performance of the "simplified bubbler" APCVD reactor. Based on results obtained in the earlier CdTe deposition, experimental emphasis was on determination of the top surface of the substrate. Thus experiments were conducted to establish the temperature of the substrate surface as a function of the temperatures of 1) substrate heater-block, 2) nozzle and 3) gas flow rate. Direct measurement using thermocouples placed on the substrate surface proved to be problematic, thus during dry runs substrate temperature was monitored using commercially available pellets with known melting points. As temperatures within the reactor were increased, researchers watched the pellets and noted the time of melting. Correlation between reactor temperatures and pellet melting points for two nozzle temperatures are shown in Figure 4.

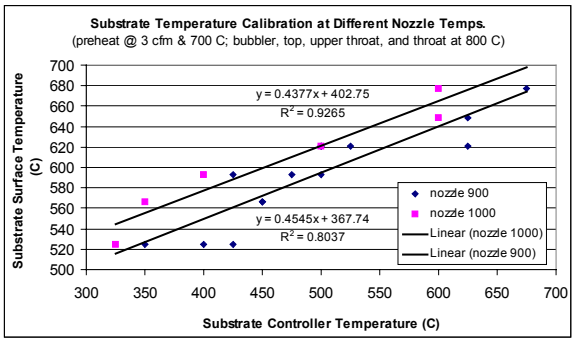

Figure 4. Representative substrate temperature calibration data from the "simplified bubbler" APCVD reactor.

3.4.7 APCVD CdTe Films and Devices – simplified reactor

Once satisfactory dry run performance had been achieved, additional reactor evaluation runs began using CdTe. First films deposited in the simplified reactor were deposited onto LOF SnO_2:F substrates using procedures intended more to investigate reactor performance than to deposit good films. Nevertheless and in spite of several deficiencies in the reactor – including a broken showerhead, the first run produced an adherent black film with characteristic feature size ~0.1 μm as shown in Figure 5. XPS depth profiling of this film indicates an oxygen content ~18 at% - possibly in the form of CdO, suggesting that there still are air leaks in the reactor.

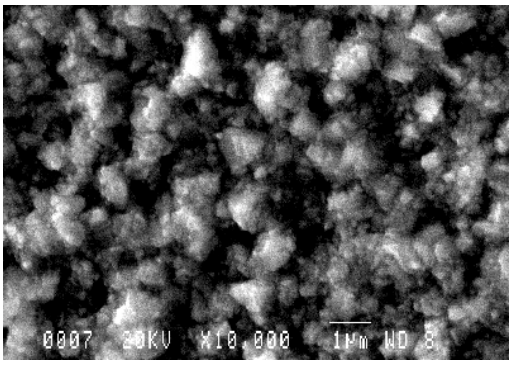

Figure 5. SEM photograph of APCVD CdTe film (Run #00214) deposited on LOF SnO_2:F.

An additional concern was the transport of CdTe particulates into the deposition zone. Particulates land on the substrate causing pinholes in the growing film. Unlike dust formation, particulates appear to have been generated within the CdTe bubbler – perhaps by rubbing together of chunks of CdTe as they were lifted and shaken by the nitrogen carrier gas - and are then transported by convection to the deposition zone. Apparently the particulates are too large, <~1 mm, to be vaporized in the hot piping. This explanation is consistent with the observation that at the end of the deposition run, particulates were observed in the hot piping between the bubbler and nozzle.

A) **B)**

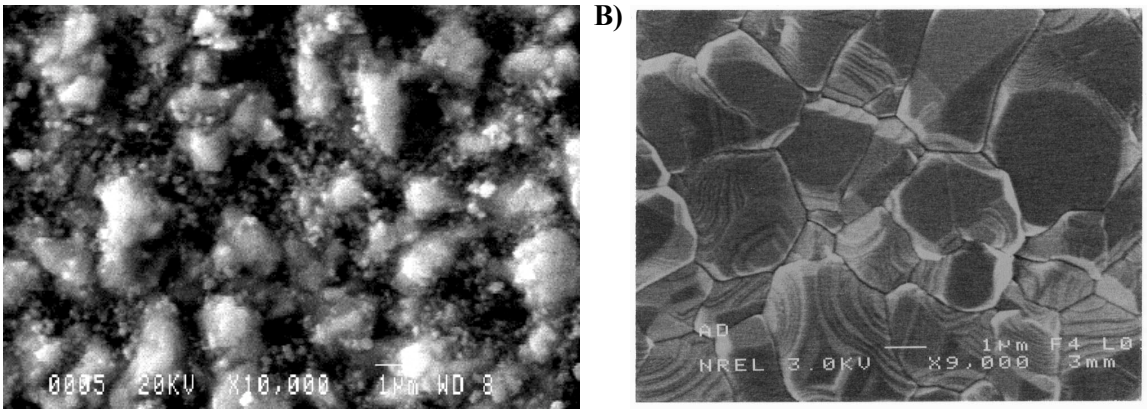

Figure 6. Comparison of A) APCVD CdTe film (Run #00222) deposited on 500 Å CBD CdS and B) CSS CdTe film deposited at NREL.

Still operating in the "shake down" mode, additional films were deposited onto thin (~500 Å) CBD CdS-coated LOF glass. Substrate temperature was estimated at 580˚C. Deposition time was about 10 minutes and film thickness varied over the range 1-4 μm . A comparison of the film structure of CdTe films from the simplified bubbler APCVD reactor and from the NREL CSS reactor is displayed in Figure 6. In spite of the preliminary nature of CdTe film deposition, Ahklesh Gupta, CSM, agreed to produce devices on the APCVD CdTe film using CSM standard processing – including a 20 min $CdCl_2$ heat treatment at 410˚C and application of evaporated Au back contacts. Best device efficiency achieved was 3.8% (373 mV Voc, 20.9 mA/cm^2 Jsc and 0.49 FF). Low Voc is attributed to the thin CdS layer that appeared to be completely consumed during CdTe deposition and processing.

3.4.8 Next Steps - Simplified Reactor

The simplified reactor has demonstrated improved control and superior films compared to the original reactor design. Specifically, no black deposits were seen on reactor windows, dust formation was primarily limited to regions outside of the substrate deposition zone, and film uniformity appears to be improved. Nonetheless, there were still significant deficiencies to be addressed including: 1) further reduction in leakage of room air into the reactor and 2) elimination of particulate flow into the deposition zone. Thus at the end of the second year, additional reactor design modifications are being developed to address these issues. Probable modifications include 1) improved joint seals and 2) insertion of particulate filters downstream of the bubbler.

4 Modeling of CdS/CdTe thin film solar cells

4.1 Device characterization and analysis

Device characterization includes measurements of film and device properties and establishment of correlations among them. Basic film properties include thickness, composition, grain size, crystallographic orientation, film stress and dark and light AC conductivity. On films deposited on CdS the composition and location of various Cd(Te,S) alloys can be determined using combinations of XRD and TEM. Device characterization includes analysis of dark and light I-V curves as well as spectral response. Measurements and analysis will be made primarily at ITN, CSM, and NREL.

A significant objective of this task is to develop a more sophisticated 2D model of device operation. Specifically, as suggested in Figure 7, the improved model is expected to include the effects of changes in composition, conductivity and carrier type associated with grain boundaries. Preliminary descriptions of this 2D model including suggested analytical validation techniques were presented at the CdTe Team meetings in May and October 1999. Validation of this model will require measurements to probe the two dimensional nature of the device. Appropriate analytical techniques to be applied include:

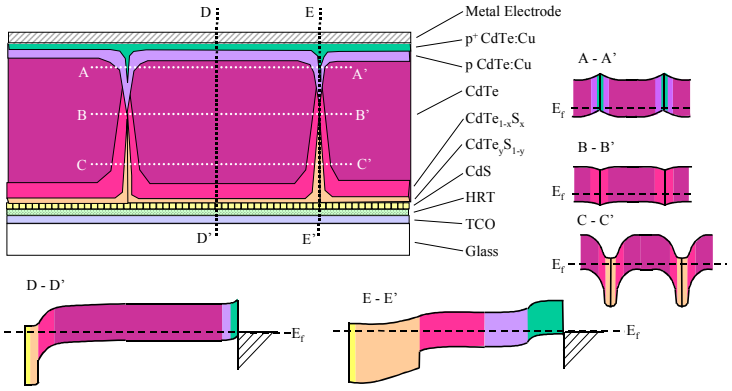

Figure 7. Schematic representation of 2-D compositional and energy level variations of an idealized polycrystalline CdTe/CdS solar cell.

1) Electrical analysis including light and dark in-plane AC impedance measurements and GB characterization of bi-crystals. These are measurements of films on relatively large scale, ~ mm, from which energy band structure around grain and grain boundaries may be inferred.

2) Microanalysis including NSOM PC, ebic, and TEM. NSOM PC measures local energy bandgap within polycrystalline films; ebic measures local electron-hole current generation; and TEM combined with EDS measures local composition, e.g., S content in CdTe.

3) Computer modeling including cross sectional 1D and 2D models enables application of measured physical parameters to models and comparison with performance of real devices.

Each approach probes device operation from a different, complementary perspective, which, when combined, are expected to define a unified representation of device operation.

4.2 AMPS Modeling of CdTe/CdS thin film PV devices[4]

4.2.1 Purposes of modeling

There are several general purposes of modeling including:

a) As a source of ideas for interpretation of measurements of materials properties and cell parameters.
b) Visualizing factors affecting carrier transport properties such as fields, carrier densities, currents, and recombination profiles, and the effects of illumination on transport in CdS/CdTe solar cells.
c) Evaluating effects of materials parameters (e.g., acceptor density) and design parameters (e.g., layer thickness) on cell operation.

An article on modeling for the CdS/CdTe cell by Burgelman et al.[5] is recommended.

The following sections include discussions of:

a) Inclusion of a CdS_xTe_{1-x} alloy layer at the CdS/CdTe interface and its effects on cell properties,
b) Preliminary model for addition of a bilayer SnO_x window to the CdS/CdTe cell,
c) Preliminary grain boundary model, and
d) Discussion of next modeling steps including two-dimensional modeling.

Associated topics in the CSU Annual Report include 1) upgrades of the AM1.5G spectrum and the absorption coefficients of CdS and CdTe used in AMPS and a comparison of AMPS and experimental spectral response curves, 2) a discussion of input parameters for AMPS modeling (especially recombination parameters), 3) effects of variation of acceptor density and minority carrier lifetime in the CdTe layer on photovoltaic performance, and 4) effects of variation of CdTe layer thickness and back contact barrier height on the on the photovoltaic variables.

A newer version AMPS-1D[6] was obtained which has the capacity to use more spectral response (SR) data points.

4.2.1.1 Choice of Parameter Values

Previous modeling used three sub-layers of CdTe with different acceptor densities (N_a) to replicate N_a profiles obtained from C-V measurements in experimental cells. Since the variations of each of the sub-layers yielded differences of only secondary magnitude, it was decided to simplify the entire CdTe layer to one N_a for this report. The measured range of N_a in real cells is 10^{13} to 10^{15} cm^{-3}, from C-V measurements.[7]

The thickness of the CdTe was chosen as 2 μm for these cases (cf., 2 to 8 μm for most experimental cells), enough to absorb virtually all sub-bandgap solar photons.

A back-contact barrier height $Ø_{bc}$ = 0.30 eV was chosen on the basis of previous modeling[8] and measurements of contact resistance vs. temperature. Above this value, the back contact barrier begins to substantially affect the ff and the J-V curves above V_{oc}.

A CdS layer thickness of 0.1 μm, a donor density $N_d = 10^{17}$ cm^{-3}, and a slightly accumulated ohmic front contact ($Ø_{fc}$ = 0.1 eV; for $N_d = 10^{17}$ cm^{-3}, $E_{CB} - E_F = 0.135$ eV), and was chosen to de-emphasize the effects of the CdS for these cases.

A summary of AMPS input parameters is given in Table 1.

Table 1. Parameter values.

	Front Contact	**SnO_x**	**n-CdS**	**p-CdS_xTe_{1-x}**	**p-CdTe**	**Back Contact**
Reflection	0.07	—	—	—	—	0.30
Barrier height (eV)	0.1	—	—	—	—	0.3, var.
Recombination. velocity, electrons (cm/sec)	10^7	—	0	0	0	10^7
Recombination. velocity, holes (cm/sec)	10^7	—	0	0	0	10^7
Thickness (μm)	—	1	0.1	0.1	2	—
Dielectric Coefficient.	—	9.0	9.0	9.4	9.4	—
Electron affinity	—	4.5	4.50	4.28	4.28	—
Band gap (eV)	—	3.1	2.42	1.41	1.50	—
Density of states, CB (cm^{-3})	—	$1.8x10^{19}$	$1.8x10^{19}$	$7.5x10^{17}$	$7.5x10^{17}$	—
Density of states, VB (cm^{-3})	—	$2.4x10^{18}$	$2.4x10^{18}$	$1.8x10^{18}$	$1.8x10^{18}$	—
Carrier density (cm^{-3})	—	10^{17}	10^{17}	10^{14}, var.	10^{14}, var.	—
Electron mobility (cm^2/V-sec)	—	350	350	500	500	—
Hole mobility (cm^2/V-sec)	—	50	50	60	60	—
Lifetime (sec)	—	$2x10^{-10}$	$2x10^{-10}$	10^{-9}	10^{-9}	—
Recombination center density N_r (cm^{-3})	—	10^{14}	10^{14}	var.	var.	—
Recombination center energy E_r (eV), wrt. VB	—	1.57	1.21	0.75	0.75	—
Recombination cross section σ_n (cm^2)	—	10^{-15}	10^{-15}	10^{-12}	10^{-12}	—
Recombination cross section σ_p (cm^2)	—	10^{-12}	10^{-12}	10^{-15}	10^{-15}	—

4.2.1.2 Target Values

Beyond being consistent with measurable materials properties (α, front and back surface optical reflection, N_d, N_a, etc.) and physical configuration (layer thicknesses, etc.), the most important requirement for a good model is to be able to duplicate the basic photovoltaic variables. For simulations of a general nature, the photovoltaic variables of the record CdS/CdTe cell of Ferekides et al.[9] were adopted. For later simulations of specific cells, their particular properties will be targets.

The simulated value of J_{sc} must be in a range consistent with the target photovoltaic variables, but it can be "fine tuned" by varying the CdS thickness (x_{CdS}, within limits of course), recombination in the CdS, and the reflection coefficients at the front and back of the cell - which are known approximately. As the specific value of Jsc is not strongly interconnected with the values of V_{oc} and ff, it was decided to focus on V_{oc} and ff and target J_{sc} separately.

On the other hand, V_{oc} and ff are strongly coupled, and for the model presented here (both in Lifetime or DOS mode), bringing V_{oc} down to target values (e.g., by decreasing τ) always resulted in a ff that was too small. Although not exhaustive, other simulations using various N_a profiles and interfacial recombination layers did not promise simultaneous targeting of V_{oc} and ff; ff was always too small if V_{oc} was targeted.

4.2.2 Addition of a CdS_XTe_{1-X} alloy layer

In this section a model was set up which includes a CdS_XTe_{1-X} alloy layer (CdSTe) at the CdS/CdTe interface, resulting from interdiffusion of S and Te and with x near the solubility limit. Such a layer is thought to be ~ 0.1 μm thick[10] with x ~ 0.04[11], giving E_g = 1.41 eV. A band offset must occur at the CdSTe/CdTe interface, either in the conduction band (ΔE_{cb}), the valence band (ΔE_{vb}), or both. Because the band offsets between CdS and CdTe occur primarily in the valence band[12], the electron affinities of CdSTe and CdTe were set to be equal, putting the discontinuity entirely in the valence band, as shown in the band diagram of Fig. 8. The lifetime $\tau = 10^{-9}$ s and $N_a = 10^{14}$ cm^{-3} were kept the same as those for the CdTe layers and the other parameters are as listed in Table 1.

The generation and total recombination for the devices with and without the CdSTe layer are shown in Fig. 9.

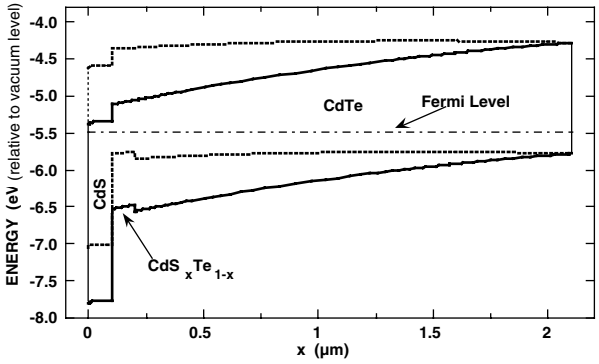

Fig. 8. Band diagram of CdSTe layer device at thermal equilibrium and at $V = V_{max}$.

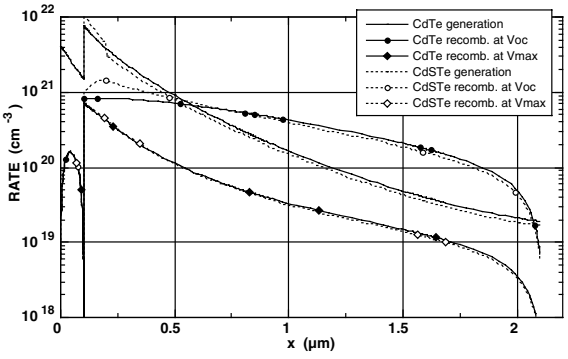

Fig. 9. Generation and recombination rates for devices with and without a CdSTe layer at V_{max} and V_{oc}.

Comparison of the generation rates for the two devices shows that the distribution of generation vs. x is moved closer to the junction for the CdSTe layer but the total generation remains similar (integration of the CdSTe/CdTe and CdTe portions of the generation curves gives 22.93 mA/cm^2 with the CdSTe and 22.37 mA/cm^2 without).

Table 2. Photovoltaic variables for CdS_xTe_{1-x} alloy layer device.

CASE	J_{sc} (mA/cm^2)	V_{oc} (V)	ff	Eff (%)
no CdSTe	24.0	0.905	0.757	16.4
ΔE_V	24.4	0.861	0.777	16.3
ΔE_C	22.8	0.804	0.664	12.2

Rather remarkably, this simple modification allows a consistent set of PV variables to be targeted. Table 2 shows these for three cases: (a) no CdSTe layer, (b) CdSTe layer as described above ("ΔE_V"), and (c) CdSTe layer with the discontinuity entirely in the conduction band ("ΔE_C"). The presence of the CdSTe layer ("ΔE_V") lowers V_{oc}, but raises the ff, leaving the efficiency almost unchanged. By adjusting the lifetime, the V_{oc} can now be adjusted to the target value (0.850 V), leaving the ff slightly above the target value (0.750), with room for slight decreases by external series resistance. The increase in ff with the CdSTe layer appears to be partially due to the movement of the generation distribution toward the junction interface, but mostly due to the decrease in V_{oc} because of the increased supply of holes for recombination near the junction interface for V = V_{oc}. As shown in Fig. 9, the recombination near the CdSTe layer increases dramatically between V_{max} and V_{oc}.

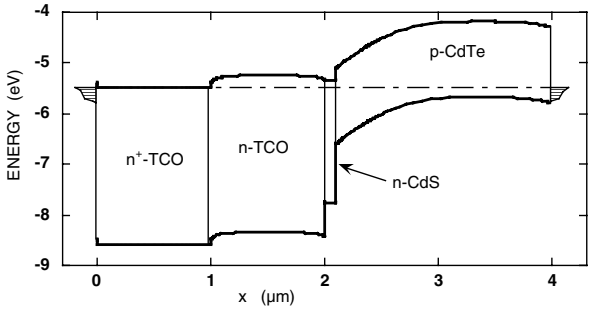

Fig. 10. Band diagram of bilayer SnO_x device. Dark, V = 0.

4.2.3 SnO_x Window layer

In this section we set up a preliminary model which includes a SnO_x window layer and describe results for situation in which the SnO_x is subdivided into layers with high and low resistivity as shown in Fig. 10. Beside the bulk photoelectronic properties of the SnO_x layers, this adds the complexity of several interfaces, each with their own interface recombination velocity as shown in Fig. 11: S_{fc}, $S_{i,hi/lo}$, $S_{i,SnOx/CdS}$. For lack of better data, the SnO_x parameters are taken as extensions of the CdS parameters (also see Table 1): the absorption coefficient of CdS is just shifted to E_g = 3.1 eV and the lifetimes are the same. Case parameters are summarized in Table 3.

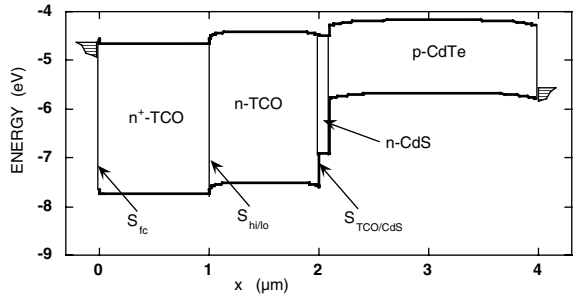

Fig. 11. Band diagram of bilayer SnO_x device. At maximum power point V = V_{max}.

Table 3. Variable parameters for SnO_x -layer cases.

	CASE	35.0	35.1	35.2	35.3
Contact	$Ø_{fc}$	0.1	0.1	0.1	0.1
Contact/SnO_x 1	$S_{fcn} = S_{fcp}$ (cm/s)	10^7	10^7	10^7	10^7
SnO_x 1	χ (eV)	4.50	**4.50**	**4.70**	**4.30**
"	x (μm)	1	1	1	1
"	N_d (cm^{-3})	10^{19}	10^{19}	10^{19}	10^{19}
SnO_x 1/SnO_x 2	$S_{hi/lo}$ (cm/s)	0	0	0	0
SnO_x 2	x (μm)	1	1	1	1
"	N_d(cm^{-3})	10^{15}	10^{15}	10^{15}	10^{15}
SnO_x 2 /CdS	$S_{SnOx/CdS}$ (cm/s)	0	0	0	0
CdS	χ (eV)	4.50	4.50	4.50	4.50
"	x (μm)	0.1	0.1	0.1	0.1
"	N_d(cm^{-3})	**10^{17}**	**10^{15}**	10^{15}	10^{15}

The SnO_x with $N_d = 10^{20}$ cm^{-3} acts essentially as an extension of the metal contact to either the more insulating SnO_x layer or the CdS and varying its thickness has little effect on the PV variables unless its S_{fc} is considered; no useful photocurrent is generated in it.

The photovoltaic variables are compared in Table 4 with an otherwise identical cell without the SnO_x layers (#32.5). The high carrier density in the CdS for this case (#35.0, $N_d = 10^{17}$ cm^{-3}) effectively shields the CdTe from influence of the SnO_x. The major difference between the two cells is the recombination velocity at the CdS front surface which was zero for the SnO_x case and $S_n = S_p = 10^7$ cm/sec for the no-SnO_x case. This results in about 1.5 mA/cm^2 increase in J_{sc}, generated in the CdS and the resultant small increases in V_{oc} and ff.

Reducing N_d in the CdS to 10^{15} moves the junction voltage drop from being almost entirely in the CdTe to being split between the CdTe and the SnO_x/CdS pair. This increases V_{oc} somewhat but decreases the ff substantially.

Table 4. SnO_x case results.

Situation	Case #	$N_{d,CdS}$ (cm^{-3})	J_{sc} (mA/cm^2)	V_{oc} (V)	ff	Eff (%)
bilayer SnO_x	35.0	10^{17}	24.58	0.956	0.784	18.4
no SnO_x	32.5	10^{17}	23.13	0.955	0.782	17.3
bilayer SnO_x	35.1	10^{15}	24.40	0.962	0.728	17.1
χ_{CdS} = 4.5, χ_{SnOx} = 4.7	35.2	10^{15}	24.19	0.961	0.622	14.4
χ_{CdS} = 4.5, χ_{SnOx} = 4.3	35.3	10^{15}	24.50	0.962	0.734	17.2

Increasing the electron affinity of the SnO_X reduces the diffusion voltage on both sides of the junction, so that the bands are bent in reverse as bias is increased near V_{max}. This reduces the light-generated current [i.e., $|J_L(V_{max})|$ is smaller for the $\chi_{SnOx} = 4.7$ eV case than for $\chi_{SnOx} = 4.7$ eV case] and results in a large reduction in ff. The dark JV curves are virtually the same for both of these cases.

Decreasing the electron affinity of the SnO_X increases the diffusion voltage on both sides of the junction, but this has little effect relative to the case for which $\chi_{SnOx} = \chi_{CdS} = 4.5$ eV. The photovoltaic variables are virtually the same for both cases.

4.2.4 AMPS grain boundary simulation

A preliminary grain boundary potential barrier model was set up in AMPS to gain insight on conditions in the CdTe parallel to the junction plane in a polycrystalline (PX) CdS/CdTe cell and how these are affected by illumination. Assumed parameters are shown in Table 5 (remaining CdTe parameters are given in Table 1). The illumination wavelength is set at 0.81–0.82 μm, which is weakly absorbed so that the photogeneration is nearly uniform throughout the CdTe, with an intensity level such that the generation is equal to that at a depth of 0.9μm into the CdTe of a CdS/CdTe cell.

Table 5. Grain boundary barrier parameters.

	Front Contact	**p-CdTe**	**n-CdTe**	**p-CdTe**	**Back Contact**
Reflection	0.07	—	—	—	0.30
Barrier height (eV)	0.1	—	—	—	0.1
Recombination. velocity, electrons (cm/sec)	10^7	—	—	—	10^7
Recombination. velocity, holes (cm/sec)	10^7	—	—	—	10^7
Thickness (μm)	—	1	0.1	1	—
Carrier density (cm^{-3})	—	10^{16}	10^{17}	10^{16}	—
Electron mobility (cm^2/V-sec)	—	350	350	350	—
Hole mobility (cm^2/V-sec)	—	60	60	60	—
Lifetime (sec)	—	10^{-9}	10^{-10}	10^{-9}	—

AMPS is not optimized for this situation and it was unable to finish the first trial case. By reducing the voltage step size (on the advice of Hong Zhu at Penn State), the case worked, but some of the results (e.g., the dark JV data) were noisy.

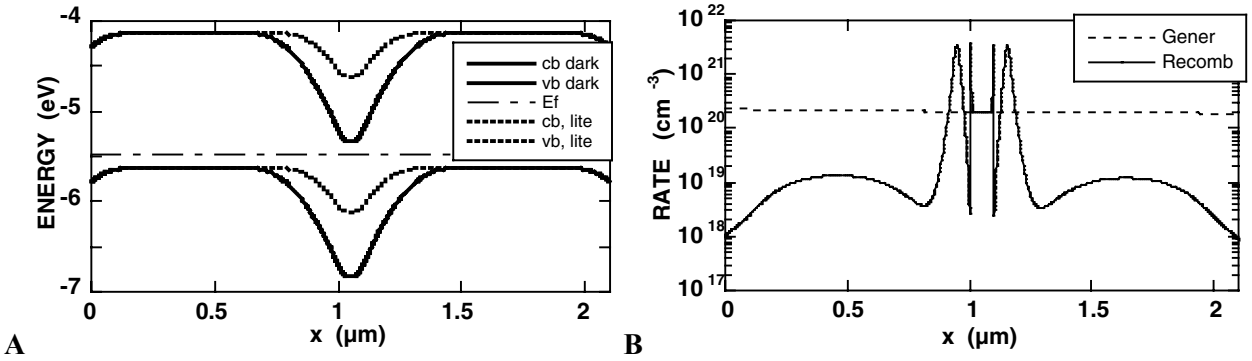

Fig. 12. (A) Grain boundary band diagram light and dark, with (B) corresponding generation and recombination profiles

Figs. 12A and 12B show the resulting band diagrams for light and dark, showing a reduction in barrier height from 1.2 to 0.50 eV (relative to valence band) with this level of illumination. The plot of recombination rate shows that the depletion layers are very efficient at collecting photogenerated carriers for recombination under the given set of assumptions.

4.2.5 AMPS modeling conclusions

- The AM1.5G spectrum and the absorption coefficients of CdS and CdTe used in AMPS were upgraded and cases are available for download by email attachment.[13]
- Insertion of a CdS_XTe_{1-X} alloy layer allows a consistent set of PV variables to be targeted exactly by small variations of reflection and CdS layer thickness for J_{sc} and variation of lifetime and the CdSTe layer thickness for V_{oc} and ff.
- Preliminary modeling of cells with TCO layers has been done, indicating the need for more experimental data on interface recombination velocities and band discontinuities.

Next steps:

- Redo the CdSTe alloy layer analysis using the DOS mode and determine sensitivity to recombination center parameters (especially Nr) in the CdSTe layer.
- Up to this point simulation has been targeted at generic cell variables. Simulation of particular cells (those with the most experimental data), hopefully following them through stressing, should be used to test and strengthen the models, and
- Refine the grain boundary model using the DOS mode, to obtain more realistic values of barrier height and then do activation energy analyses.

5 Summary

5.1 Phase II Summary

Activities during the second year of the APCVD program were directed toward improved design and testing of the APCVD reactor. Fabrication of the first generation stagnant flow reactor was completed and the first APCVD CdTe was deposited. Deficiencies in the original design were identified and the ITN/CSM team designed, built and tested a “simplified bubbler” reactor that addressed deficiencies discovered in the original design. Perhaps the most significant result of Phase II, however, was that by depositing adherent, coherent CdTe films researchers provided strong evidence to support the

fundamental premise of this program – that APCVD has the same reaction chemistry – and presumably the same potential for producing high efficiency devices, as does CSS.

Accomplishments during the Phase II include:

- Deposition of the first APCVD CdTe films
- Fabrication of the first APCVD CdTe PV devices
- Identification and correction of deficiencies in the Phase I APCVD reactor
- Modeling effects on CdTe device performance of CdSTe, TCO bi-layers and grain boundaries

5.2 Planned Phase III activities

During Phase III ITN plans to develop operating procedures which optimize performance of the simplified bubbler and to produce device quality films uniformly over 64 cm^2 area. At the same time reactor performance will be evaluated in order to establish engineering parameters required for the design of a more advanced reactor. While only minor modifications to the simplified bubbler are anticipated, ITN and its team intend to utilize knowledge gained from analysis of simplified bubbler performance to build a second-generation laboratory scale reactor which includes provision for substrate transport and steady state operation.

5.3 Planned third year milestones

During the third year of the program ITN expects to meet the following milestones as called for in the original subcontract:

- Demonstration of device quality CdTe films.
- Demonstrate control of film properties over 64 cm^2 area
- Demonstration of 15% power conversion efficiency on a 1 cm^2 cell.
- Demonstrate CdTe-specific 2D model with measurements to validate model
- Identify grain boundary factors affecting device efficiency and demonstrate their effects through analysis of a working device

6 References

1 C. Ferekides and J. Britt, Solar Energy Mat. & Solar Cells 35 (1994) pp 255-262.

2 H. Ohyama, T. Aramoto, S. Kumazawa, H. Higuchi, T. Arita, S. Shibutani, T. Nishio, J. Nakajima, M. Tsuhi, A. Hanafusa, T. Hinino, K. Omura, and M. Murozono, "16.0% Efficient Thin-Film Solar Cells", Proc. 26th PVSC (1997) pp 343-346.

3 P.V. Meyers and R.W. Birkmire, Prog. in PV:Res. & Appl., Vol 3 (1995) pp 393-402.

4 Section prepared by Alan Fahrenbruch, ALF.

5 M. Burgelman, P. Nollet, and S. Degrave, Thin Solid Films 361-362, 527 (00) (special issue on E-MRS Conf., Symposium O: Chalcogenide semiconductors for Photovoltaics).

6 Modeling results were obtained using AMPS-1D, version 1,0,0,1, written under the direction of S. Fonash at Pennsylvania State University and supported by the Electric Power Research Institute.

7 See, for example, J. Hiltner and J. Sites, NCPV Program Review, AIP Conf. Proc. 462 (1998) p. 170 and D. Rose, D. Rose, First Solar, CdTe Team Meeting, 9/8/98.

8 See, for example, J. Sites, Annual Report (1994), NREL Subcontract XAX-4-14000-01, p. 6 and A.L. Fahrenbruch, NCPV Program Review, AIP Conf. Proc. 462 (1998) p. 48.

9 C. Ferekides et al., Proc. 23rd IEEE PV Spec. Conf. (1993) p. 389. Jsc = 25 mA/cm^2, Voc = 0.85 V, ff = 0.75, and Eff = 15.8%.

10 Brian McCandless, IEC, personal communication.

11 D.G. Jensen, B.E. McCandless, and R.W. Birkmire, Proc. 25th IEEE PVSC (1996) pp 773-776.
12 Su-Huai Wei and Alex Zunger, Appl. Phys. Lett., **72**, 2011 (1998) and Su-Huai Wei S.B. Zhang, and Alex Zunger, J. Appl. Phys., **87**, 1304 (2000).
13 Representative AMPS case files will be sent on email request to Alan Fahrenbruch <alanf@stanford.edu>.

REPORT DOCUMENTATION PAGE

Form Approved
OMB NO. 0704-0188

1. AGENCY USE ONLY (Leave blank)	2. REPORT DATE	3. REPORT TYPE AND DATES COVERED
	May 2000	Annual Subcontract Report, 26 January 1999–25 January 2000

4. TITLE AND SUBTITLE
Atmospheric Pressure Chemical Vapor Deposition of CdTe for High Efficiency Thin Film PV Devices; Annual Subcontract Report, 26 January 1999–25 January 2000

5. FUNDING NUMBERS
C: ZAK-8-17619-03
TA: PV005001

6. AUTHOR(S)
P.V. Meyers, R. Kee, C. Wolden, J. Kestner, L. Raja, V. Kaydanov, T. Ohno, R. Collins, and A. Fahrenbruch

7. PERFORMING ORGANIZATION NAME(S) AND ADDRESS(ES)
ITN Energy Systems
12401 W. 49th Ave.
Wheat Ridge, CO 80033

8. PERFORMING ORGANIZATION REPORT NUMBER

9. SPONSORING/MONITORING AGENCY NAME(S) AND ADDRESS(ES)
National Renewable Energy Laboratory
1617 Cole Blvd.
Golden, CO 80401-3393

10. SPONSORING/MONITORING AGENCY REPORT NUMBER
SR-520-28375

11. SUPPLEMENTARY NOTES
NREL Technical Monitor: H.S. Ullal

12a. DISTRIBUTION/AVAILABILITY STATEMENT
National Technical Information Service
U.S. Department of Commerce
5285 Port Royal Road
Springfield, VA 22161

12b. DISTRIBUTION CODE

13. ABSTRACT *(Maximum 200 words)*
ITN's three-year project, Atmospheric Pressure Chemical Vapor Deposition (APCVD) of CdTe for High Efficiency Thin-Film PV Devices, has the overall objectives of improving thin-film CdTe PV manufacturing technology and increasing CdTe PV device power conversion efficiency. CdTe deposition by APCVD employs the same reaction chemistry as has been used to deposit 16%-efficient CdTe PV films, i.e., close-spaced sublimation, but employs forced convection, rather than diffusion, as a mechanism of mass transport. Tasks of the APCVD program center on demonstration of APCVD of CdTe films, discovery of fundamental mass transport parameters, application of established engineering principles to the deposition of CdTe films, and verification of reactor design principles that could be used to design high-throughput, high-yield manufacturing equipment. Additional tasks relate to improved device measurement and characterization procedures that can lead to a more fundamental understanding of CdTe PV device operation, and ultimately, to higher device conversion efficiency and greater stability. Under the APCVD program, device analysis goes beyond conventional one-dimensional device characterization and analysis toward two-dimensional measurements and modeling. Accomplishments of the second year of the APCVD subcontract include: deposition of the first APCVD CdTe; identification of deficiencies in the first-generation APCVD reactor; design, fabrication, and testing of a "simplified" APCVD reactor; deposition of the first dense, adherent APCVD CdTe films; fabrication of the first APCVD CdTe PV device; modeling effects of CdSTe and SnO_x layers; and electrical modeling of grain boundaries.

14. SUBJECT TERMS
photovoltaics ; atmospheric pressure chemical vapor deposition ; APCVD ; cadmium telluride ; CdTe ; reactors ; thin-film solar cells ; modeling ; grain boundaries ; Thin Film PV Partnership

15. NUMBER OF PAGES

16. PRICE CODE

17. SECURITY CLASSIFICATION OF REPORT	18. SECURITY CLASSIFICATION OF THIS PAGE	19. SECURITY CLASSIFICATION OF ABSTRACT	20. LIMITATION OF ABSTRACT
Unclassified	Unclassified	Unclassified	UL